Analysis of Electrostatic and Hydrophobic Complementarities Between Chymotrypsin and Avian Ovomucoid Third Domains Using Molecular Electrostatic Potential: Effect of Residue Replacements

HIDEO NAKAJIMA and OSAMU KIKUCHI*

Department of Chemistry, University of Tsukuba, Tsukuba 305, Japan

Received August 14, 1995; accepted November 29, 1995

ABSTRACT

Electrostatic and hydrophobic complementarities between chymotrypsin and its inhibitor, avian ovomucoid third domains, were evaluated for eight species, which have different amino acid sequences, using molecular electrostatic potential (MEP) and MEP correlation, and the enzyme–inhibitor interaction was analyzed. The changes in the electrostatic and hydrophobic complementarities caused by the amino acid replacements were reflected clearly in the calculated MEP correlation, and it explained the observed binding association constants correctly. The electrostatic complementarity due to arginine at P_3' strongly promotes the binding process of the inhibitor, while the hydrophobic complementarity in the P_1 and P_2' positions also affects the binding process. It was demonstrated that our method is an effective molecular modeling tool in drug design and protein engineering. © 1996 John Wiley & Sons, Inc.

Introduction

Chymotrypsin is one of the enzymes most widely studied [1,2] and its three-dimensional structure was determined by X-ray crystallography [3]. It catalyses the rupture of the peptide bond caused by a nucleophilic attack of Oγ of Ser 195. Ovomucoid inhibitors are major components of avian egg whites and are responsible for most of the inhibitory activity against serine proteases in the egg white. Generally, they consist of three tandem domains, each of which is an inhibitor of serine proteases and belongs to the family of Kazal

*To whom correspondence should be addressed.

CCC 0020-7608 / 96 / 051081-11

inhibitors [4–6]. The mechanism of interaction between an enzyme and an inhibitor can be expressed by the equation [6–8]

$$E + I \rightleftharpoons C \rightleftharpoons E + I^*, \tag{1}$$

where E is the enzyme, I and I^* are the virgin and modified inhibitors, respectively, and C is a stable complex. The binding equilibrium constant

$$K_a = \frac{[C]}{[E][I]} \tag{2}$$

is a measure of the interaction; a good inhibitor easily forms a stable complex with an enzyme and has a large K_a value. A large number of third domains of various avian species were isolated and sequenced by Laskowski et al. [8–10]. The effect of the amino acid substitution on the K_a value was compared and it was shown that the changes in the primary contact regions exert large effects on the K_a value [8]. The X-ray structure of the complex of chymotrypsin and turkey ovomucoid third domain was determined [11].

In the enzyme–substrate interactions, electrostatic and hydrophobic interactions are important for a successful binding of a substrate [12]. The electrostatic interaction is often explained by means of the electrostatic complementarity which is the matching of the electrostatic properties created by the enzyme and the substrate. When electrostatic properties of a molecule are expressed by the molecular electrostatic potentials (MEPs) [13–15], the electrostatic complementarity is represented by the MEP correlation which is the product of the MEPs created by the enzyme and the substrate [16]; a large negative value means a large electrostatic stabilization. Hydrophobic stabilization is seen between nonpolar fragments in the enzyme–substrate system. The hydrophobic complementarities between guest ligands and host enzymes were discussed by Naray-Szabo et al. [15, 17]. The hydrophobic effect is the consequence that the nonpolar regions tend to come together to escape contact with water and to minimize the dehydration free energies. Since an affinity for a certain region to form a hydrogen bond with a water molecule can be regarded as proportional to the MEP [18], the hydrophobic complementarity also can be expressed indirectly by the MEPs of the enzyme and the substrate; a small MEP correlation corresponds to a large hydrophobic stabilization. Therefore, both electrostatic and hydrophobic complementarities can be analyzed on the basis of the MEPs of the enzyme and the substrate.

To evaluate the MEP of a molecule, the electron-density distribution is needed. However, it is difficult to obtain the SCF-MOs and the electron-density functions for large molecules like proteins. The point charge models are sometimes used in the evaluation of the MEPs of enzymes [19, 20]. Although they are simple and require less computation time, their MEPs diverge near each point charge and are reliable only at a long distance from each nucleus in a molecule. Furthermore, the models hardly reproduce the directional property of the MEP due to long-pair electrons. We proposed a set of simple empirical functions [21, 22] which can be used for the systematic evaluation of reliable MEPs of proteins with very short computation time. The method reproduces well the MEP change due to a conformational change of a molecule.

In this article, the chymotrypsin–ovomucoid interactions are analyzed using electrostatic and hydrophobic complementarities. The MEPs of the enzyme and the inhibitors were calculated by using our simple functions whose parameters were recently determined [22]. The complementarities were evaluated by the MEP and the MEP correlations for eight species of the ovomucoids that have different amino acid sequences. The effect of residue replacements on the chymotrypsin–ovomucoid interactions is discussed in relation to the observed binding equilibrium constants, K_a.

Methods and Materials

EVALUATION OF MEP

The MEP at a point $\mathbf{r}$ is given by

$$V(\mathbf{r}) = \frac{1}{\varepsilon}\sum_A \frac{Z_A}{|\mathbf{r} - \mathbf{r}_A|} - \frac{1}{\varepsilon}\int \frac{\rho(\mathbf{r}')}{|\mathbf{r} - \mathbf{r}'|}\, d\mathbf{r}'$$
$$= V_{core}(\mathbf{r}) + V_{elec}(\mathbf{r}), \tag{3}$$

where ε is the dielectric constant of a medium; Z_A, the nuclear charge of atom A; $\mathbf{r}_A$, the position of atom A; and $\rho(\mathbf{r}')$, is the electron-density function at $\mathbf{r}'$. The first term in Eq. (3), $V_{core}(\mathbf{r})$, corresponds to the positive contribution from the nuclei, and the second term, $V_{elec}(\mathbf{r})$, to the negative contribution from the electrons.

In the present method, electrostatic potentials (EPs) due to electrons in the valence shells are calculated by a set of simple functions, $F_i(\mathbf{r})$, at various origins, while those due to the core electrons and nuclei by point charge approximation,

$$V(\mathbf{r}) = V_{core}(\mathbf{r}) + \frac{1}{\varepsilon}\sum_{i}^{occ} n_i F_i(\mathbf{r}) \tag{4}$$

$$F_i(\mathbf{r}) = -\sum_j \frac{q_j}{\left[|\mathbf{r} - \mathbf{r}_j|^2 + a_j \exp\left(-b_j|\mathbf{r} - \mathbf{r}_j|^2\right)\right]^{1/2}}, \tag{5}$$

where n_i is the occupation number of the ith orbital. The EPs of σ and lone-pair orbitals were approximated by three functions ($j = 3$) and π orbitals by six functions ($j = 6$). The origins of the functions of σ and lone-pair orbitals, $\mathbf{r}_j$, were located on the symmetrical axis of the orbital. For π orbitals, two of the $\mathbf{r}_j$ were located on the symmetrical axes of the $2p\pi$ atomic orbitals of the two atoms which compose the π bond, and the third origin is above the center of the two atoms. Another set of three origins are placed below the molecular plane symmetrically: thus, a total six functions were used. q_j is the electron population assigned at jth origin. The parameters a_j, b_j, q_j, and $\mathbf{r}_j$ were determined by least-square fitting between the EP of the STO-5G basis set [23] and that calculated by the function $F_i(\mathbf{r})$. The parameters required for the evaluation of the MEPs of the enzyme and inhibitors were reported [22], and the same parameters were used in this study. The detailed procedure for the MEP calculation was reported in previous articles [21, 22].

For the dielectric constant, ε, we used the distance-dependent sigmoidal function [24],

$$\epsilon(R) = D - \left[\frac{D-1}{2}\right] \times \exp(-RS)[(RS)^2 + 2RS + 2], \tag{6}$$

where R is the distance between the point $\mathbf{r}$ where the MEP is calculated and the position of atom A or the origin of the MEP function; S, the parameter which represents the slope of the function; and D, the maximum value of ε. We set $S = 0.3$ as in the literature [24] and $D = 4$ as the internal dielectric constants of a protein [20, 25].

MEP CORRELATION AND THE MEASURE OF THE COMPLEMENTARITIES

The MEP correlation at a point $\mathbf{r}$, $E_c(\mathbf{r})$, is defined as [16]

$$E_c(\mathbf{r}) = \text{sign}(V_e(\mathbf{r}) \cdot V_i(\mathbf{r}))[V_e(\mathbf{r}) \cdot V_i(\mathbf{r})]^{1/2}, \tag{7}$$

where $V_e(\mathbf{r})$ denotes the MEP of a host enzyme, and $V_i(\mathbf{r})$, of a guest inhibitor. Thus, electrostatic stabilization occurs in the region with negative $E_c(\mathbf{r})$, where $V_e(\mathbf{r})$ and $V_i(\mathbf{r})$ have signs opposite to each other and destabilization occurs in the region with positive $E_c(\mathbf{r})$. $E_c(\mathbf{r})$ was evaluated on the van der Waals surface of the inhibitor. Their points were taken at 0.1 Å spacing. To examine the effect of residue replacements, we defined the MEP correlation of each residue of the inhibitor, $E_{c,res}$,

$$E_{c,res} = \frac{1}{N_s}\sum_{i=1}^{n_s} E_c(r_i), \tag{8}$$

where N_s is the number of the total points on the van der Waals surface of the inhibitor and n_s is that of the residue. $E_{c,res}$ is a measure of the electrostatic complementarity at each residue of the inhibitors. The 3-D MEP correlation was also calculated around the inhibitor and its map was compared for several species.

The absolute value of the $E_c(\mathbf{r})$ was regarded as the index of hydrophobicity, since it represents the strength of the MEPs of the enzyme and the inhibitors. Its averaged value of a residue, $F_{c,res}$ defined by

$$F_{c,res} = \frac{1}{n_s}\sum_{i=1}^{n_s} |E_c(r_i)|, \tag{9}$$

is a measure of the hydrophobic complementarity at each residue of the inhibitors. (Note that the denominator is n_s, not N_s.) The hydrophobic interaction is large where $F_{c,res}$ is small. Chothia showed that the reduction of the solvent accessible surface area correlates with the hydrophobic free energies [26]. It was also used for the determination of the hydrophobic region. The solvent-accessible surface was calculated as done by Lee and Richards [27]. Thus, we considered the two requirements for a favorable hydrophobic interaction: a small $F_{c,res}$ value and a large overlapped area of the solvent-accessible surface.

TABLE I
Residues of the active site of chymotrypsin which are located within 9 Å from the Oγ of Ser 195 and which contact with turkey ovomucoid third domain within 6 Å.

Asp 35	Asp 64	Trp 172	Ile 212
			Val 213
His 40	Tyr 94	Lys 175	Ser 214
Phe 41			Trp 215
Cys 42	Ile 99	Ser 189	Gly 216
Gly 43		Ser 190	Ser 217
	Asp 102	Cys 191	Ser 218
Ala 55		Met 192	Thr 219
Ala 56	Leu 143	Gly 193	Cys 220
His 57		Asp 194	
Cys 58	Ala 149	Ser 195	Gly 226
Gly 59	Asn 150	Gly 196	Val 227
Val 60	Thr 151	Gly 197	Tyr 228

MODELS OF THE ENZYME AND INHIBITORS

The atomic coordinates of the enzyme and the inhibitors were obtained from the crystal structure of the chymotrypsin and turkey ovomucoid complex [11] provided by the Brookhaven Protein Data Bank. All atoms in the enzyme were included for the MEP calculation. The MEP and MEP correlation maps are shown around the active site of the enzyme whose amino acids are listed in Table I. The active site was described by 42 amino acids which are located within 9 Å from the Oγ of the active serine (Ser 195) and which contact with the inhibitor within the distance of 6 Å. For the inhibitor, the primary contact region, P_6–P'_3,[†] was considered. Aspartate, glutamate, lysine, and arginine were treated in their ionic forms. The amino acid sequences and the K_a values of the eight ovomucoids involved in this study are listed in Table II. The NH and CO groups which were artificially created at the end of the inhibitor were converted into the NH_2 and COH groups, respectively. The structures for the enzyme–ovomucoid complexes other than that for turkey were obtained by replacing the corresponding amino acids. The coordinates of the newly introduced amino acids and its contact part of the enzyme were optimized with the AM1 MO calculation [29] using our MOSEMI program.

Results and Discussion

MEP MAP OF CHYMOTRYPSIN

The 3-D MEP map of chymotrypsin is shown in Figure 1. It has three negative clouds around (i) Asp 102, which plays an important role in its catalytic process [30]; (ii) Asp 194, which makes an atmosphere of the binding site near P_1 and P'_2 region of the inhibitor; and (iii) Asp 35 and Asp 64, which make a highly negative binding site at P'_3. Thus, electropositive binding sites are located from

[†]In designing the position of an amino acid in the inhibitor relative to the scissile bond and its corresponding binding site of the enzyme, the terminology of Schechter and Berger [28] was used. The nomenclature ($P_n, \ldots, P_2, P_1, P'_1, P'_2, \ldots, P'_n$) denotes the amino acid residues of the inhibitor, where P_1–P'_1 is the scissle bond. ($S_n, \ldots, S_2, S_1, S'_1, S'_2, \ldots, S'_n$) are the corresponding binding sites of the enzyme.

TABLE II
Amino acid sequences of ovomucoid third domains.[a]

Species of ovomucoid	P_6	P_5	P_4	P_3	P_2	P_1	P'_1	P'_2	P'_3	K_a[b]
Turkey	Lys	Pro	Ala	Cys	Thr	Leu	Glu	Tyr	Arg	3.2×10^{11}
Chestnut bellied scaled quail	Lys	Pro	*Asp*	Cys	Thr	Leu	Glu	Tyr	Arg	5.9×10^{11}
Silver pheasant	Lys	Pro	Ala	Cys	Thr	*Met*	Glu	Tyr	Arg	1.8×10^{11}
Indian peafowl	Lys	Pro	Ala	Cys	Thr	Leu	Glu	*His*	Arg	1.3×10^{10}
Chicken	Lys	Pro	*Asp*	Cys	Thr	*Ala*	Glu	*Asp*	Arg	1.9×10^{3}
Duck	Lys	Pro	Ala	Cys	Thr	*Met*	Glu	Tyr	*Met*	1.5×10^{10}
Goose	Lys	Pro	Ala	Cys	Thr	*Val*	Glu	Tyr	*Met*	1.8×10^{4}
Rhea	Lys	Pro	*Val*	Cys	*Ser*	Leu	Glu	Tyr	*Met*	8.9×10^{7}

[a]Amino acids which are replaced from turkey ovomucoid are shown in italics.
[b]From [6, 8]. Values are in M^{-1}.

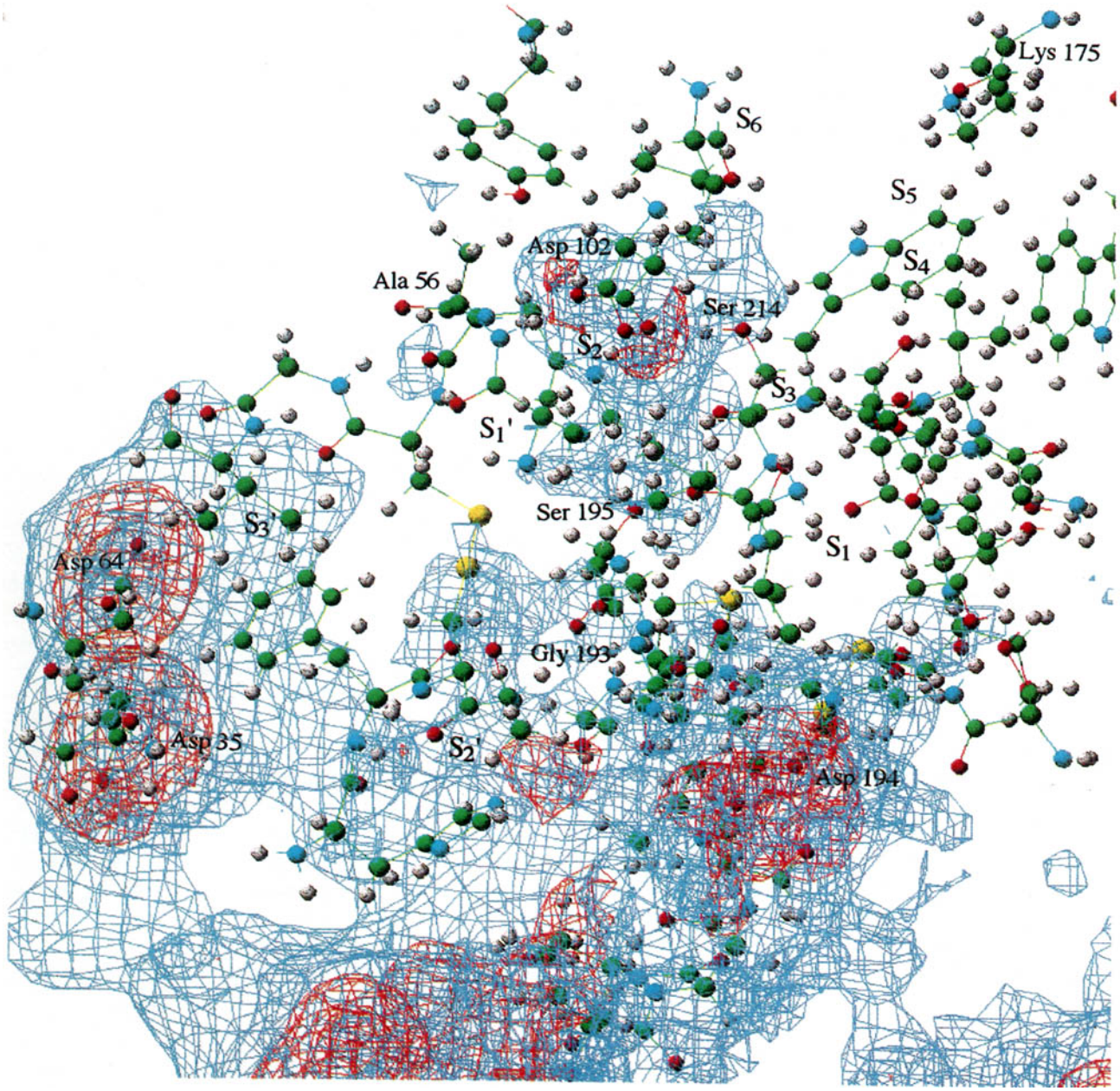

FIGURE 1. 3-D MEP map of chymotrypsin in the active site. The active site of the enzyme (Table I) is shown in the ball and stick model. Green, red, blue, and gray atoms are carbon, oxygen, nitrogen, sulfur, and hydrogen, respectively. Isosurfaces were taken at the -120 kcal mol^{-1} (red) and -60 kcal mol^{-1} (blue) levels.

S_6 to S_3, while electronegative sites are S_2 to S_3'. The S_1 binding pocket of chymotrypsin was explained as a hydrophobic site, and, in fact, the substrate which has a hydrophobic residue has a large affinity [2]. However, the facts that (i) no avian ovomucoid has a residue having a negative charge at the P_1 region [9], (ii) the bobwhite quail ovomucoid third domain which has a serine residue at P_1 is an inactive inhibitor of α-chymotrypsin [7], and (iii) soybean trypsin inhibitors which have an arginine residue at P_1 inhibits α-chymotrypsin [31] may lead us to the validity of the negative MEP near the S_1 binding pocket.

COMPLEMENTARITY BETWEEN CHYMOTRYPSIN AND TURKEY OVOMUCOID THIRD DOMAIN

The calculated $E_{c,res}$ and $F_{c,res}$ values are listed in Tables III and IV, respectively. The comparison of the overlapped area of the solvent accessible surface of the ovomucoids is provided in Table V.

Figure 2 shows the 3-D MEP correlation map of turkey ovomucoid. A large negative cloud is seen at P'_3. It is due to the negative MEP around Asp 35 and Asp 64 of the enzyme and the positive MEP of Arg 21 of the inhibitor. On the other hand, positive clouds were seen around P'_1 and around P_5 and P_6. The former is due to the negative MEP of Asp 102 of the enzyme and that of Glu 19 of the inhibitor, and the latter is caused by the positive MEP of Lys 175 of the enzyme and that of Lys 13 of the inhibitor. The negative cloud around P'_3 plays an important role in the binding process of this inhibitor. From Tables IV and V, it is seen that the P_1 and P'_2 positions have small $F_{c,res}$ and large overlapped area of the solvent-accessible surface. Thus, hydrophobic interaction is dominant at P_1 and P'_2.

CHESTNUT BELLIED SCALED QUAIL OVOMUCOID

The first comparison is that of an alanine–aspartate change (turkey–chestnut bellied scaled quail) in the sequence position P_4. The change creates a negative cloud around P_4 and P_5. It is due to the positive MEP of Lys 175 and the negative MEP of the introduced aspartate of the inhibitor. As seen in Table III, the MEP correlations are highly negative at P_4 and P_5, and the total MEP correlation of the inhibitor also becomes highly negative, indicating a strong interaction between the enzyme and chestnut bellied scaled quail ovomucoid. The effect is also seen in $E_{c,res}$ and $F_{c,res}$ values of other regions; increase of $F_{c,res}$ at P_1 indicates a slight reduction of the hydrophobic complementarity in this region. However, with all this reduction of hydrophobic complementarity, the large increase of the electrostatic complement at P_4 and P_5 promotes the binding process of the inhibitor.

INDIAN PEAFOWL OVOMUCOID

The exchange of tyrosine at P'_2 for histidine (turkey–Indian peafowl) causes little effect on the electrostatic complementarity; their difference of the total MEP correlation and that of $E_{c,res}$ at P'_2 are small (Table III). However, evident change was observed in the hydrophobic complementarity (Tables IV and V). The electrostatic potential of the side chain of histidine, which is stronger than that of tyrosine, makes $F_{c,res}$ larger in Indian peafowl ovomucoid. Moreover, the overlapped area of the solvent accessible surface at P'_2 is reduced. The replacement is unfavorable for the hydrophobic interaction, and the binding of the inhibitor is discouraged. This is consistent with the K_a value which is smaller in Indian peafowl ovomucoid.

TABLE III
MEP correlation, $E_{c,res}$, between chymotrypsin and ovomucoid.

Ovomucoid species	P_6	P_5	P_4	P_3	P_2	P_1	P'_1	P'_2	P'_3	Total
Turkey	4.7	1.8	1.1	0.0	0.2	0.3	2.3	−2.3	−7.5	0.5
Chestnut bellied scaled quail	2.0	−3.4	*−5.4*	−0.2	1.2	1.1	2.7	−1.5	−7.0	−10.5
Silver pheasant	4.8	1.8	1.1	−0.1	0.1	*0.2*	2.3	−2.3	−7.5	0.4
Indian peafowl	4.8	1.8	1.1	0.0	0.2	0.3	2.3	*−2.5*	−7.8	0.1
Chicken	1.8	−4.1	*−6.2*	−0.3	2.1	*0.8*	4.1	*5.1*	−5.4	−2.1
Duck	4.6	1.5	0.9	−0.1	0.7	*0.9*	4.0	0.6	2.2	15.3
Goose	4.7	1.5	0.9	−0.1	0.8	*0.6*	4.0	0.6	*2.3*	15.2
Rhea	4.6	1.5	*1.6*	−0.1	*1.0*	0.9	3.9	0.5	*2.2*	16.0

Values are in kcal mol^{-1}. For the replaced position from turkey ovomucoid, values are shown in italics.

TABLE IV
Absolute MEP correlation $F_{c,res}$, between chymotrypsin and ovomucoid.

Ovomucoid species	P_6	P_5	P_4	P_3	P_2	P_1	P'_1	P'_2	P'_3
Turkey	39.5	32.4	23.4	15.1	27.1	21.1	33.7	22.9	50.7
Chestnut bellied scaled quail	34.1	41.7	*64.4*	16.3	24.5	23.3	35.2	21.3	49.6
Silver pheasant	39.6	32.4	23.5	14.6	27.2	*21.2*	33.6	22.8	50.7
Indian peafowl	39.5	32.4	23.4	15.1	27.1	21.1	33.5	*29.9*	51.1
Chicken	33.7	44.4	*66.5*	17.6	25.6	*30.1*	39.6	*54.6*	47.5
Duck	38.6	30.6	21.9	15.0	26.2	*22.6*	39.5	20.6	*23.5*
Goose	38.6	30.6	21.7	15.4	26.4	*24.8*	39.8	20.6	*23.5*
Rhea	38.7	31.0	*22.5*	15.3	*27.2*	22.3	39.1	20.5	*23.4*

Values are in kcal mol^{-1}. For the replaced position from turkey, values are shown in italics.

CHICKEN OVOMUCOID

Chicken ovomucoid differs from chestnut bellied scaled quail in two positions: Alanine and aspartate occur at P_1 and P'_2 instead of leusine and tyrosine, respectively. As shown in Table III, the change into aspartate at P'_2 causes large electrostatic destabilization. As a result, the total MEP correlation of chicken ovomucoid is decreased by 8 kcal mol^{-1} from that of chestnut bellied scaled quail. Also, those replacements ruin the hydrophobic complementarities at P_1 and P'_2. Aspartate introduced at P'_2 makes the $F_{c,res}$ values of P_1 and P'_2 large (Table IV). Furthermore, the overlapped area of the solvent-accessible surface is reduced considerably at P_1 and P'_2 (Table V). Thus, the hydrophobic interactions in these regions are strongly reduced. It is suggested that chicken ovomucoid is the most inactive of the eight species. Its large reduction of the K_a value can be explained by the loss of electrostatic complementarity at P'_2 and by the large reduction of the hydrophobic complementarity at P_1 and P'_2.

METHIONINE AT P'_3

The most dramatic change of the electrostatic complementarity was observed on the P'_3 replacement of arginine into methionine. For example, the 3-D MEP correlation map of goose ovomucoid is shown in Figure 3. It differs from turkey ovomucoid in two positions: It has valine at P_1 instead of leusine and methionine at P'_3 instead of arginine (Table II). The replacement at P'_3 creates a large positive cloud in this region. As shown in Figure 1, the MEP of the enzyme is strongly electronegative due to Asp 35 and Asp 64 in this region, and the

TABLE V
Comparison of the overlapped area of the solvent-accessible surface of the ovomucoids.

Ovomucoid species	P_6	P_5	P_4	P_3	P_2	P_1	P'_1	P'_2	P'_3
Turkey	0.006	0.043	0.041	0.034	0.058	0.118	0.044	0.098	0.064
Chestnut bellied scaled quail			1.251						
Silver pheasant						1.008			
Indian peafowl								0.846	
Chicken			1.251			0.581		0.680	
Duck						1.008			0.317
Goose						0.840			0.317
Rhea			1.431		0.666				0.317

The overlapped area of turkey ovomucoid was evaluated as $S_{overlap} = n_s / N_{total}$, where n_s is the number of the overlapped surface points of a residue, and N_{total}, the number of the total surface points of an inhibitor. These points were taken at 0.1 Å spacing on the solvent-accessible surface. For other ovomucoids, the ratios of the number of points to the turkey are shown only for the replaced positions.

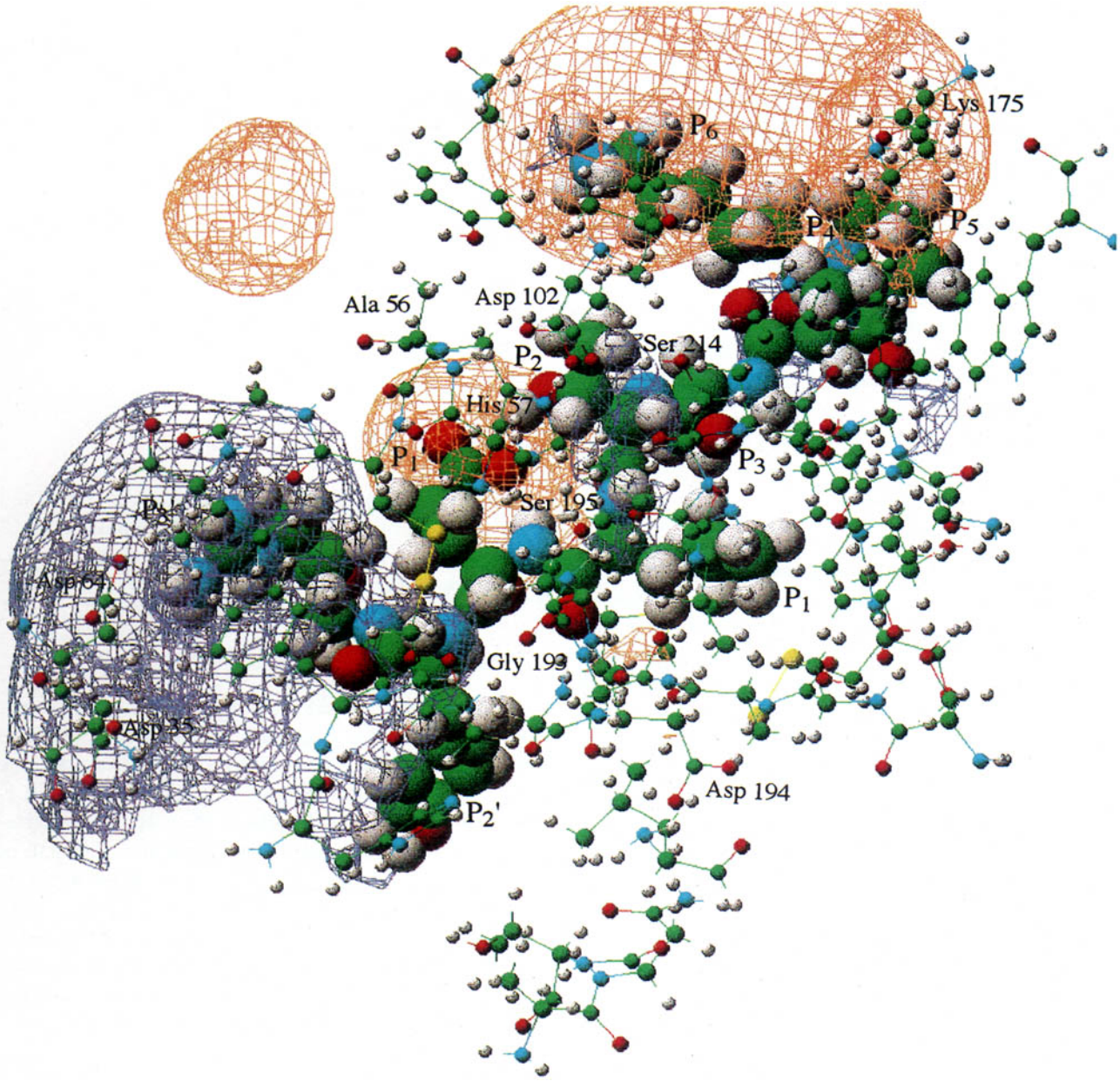

FIGURE 2. 3-D MEP correlation map of turkey ovomucoid. The active site of the enzyme (Table I) is shown in the ball and stick model, and the primary contact regions of turkey ovomucoid are shown by the space-filling model. The colors of the atoms are same as Figure 1. Isosurfaces were taken at the -30 kcal mol^{-1} (purple) and $+30$ kcal mol^{-1} (orange) levels.

positive MEP of P_3' arginine has a large effect on electrostatic stabilization. Hence, the replacement of arginine into neutral methionine removes large attractive interaction between the enzyme and the inhibitor and causes a reduction of the K_a value. It can be said that the electrostatic complementarity at P_3' has an important role for the successful binding of the inhibitor. This result is reflected in small K_a values of rhea and goose ovomucoids. The difference between these ovomucoids can be explained well by the difference in hydrophobic complementarity at P_1 as in the next section.

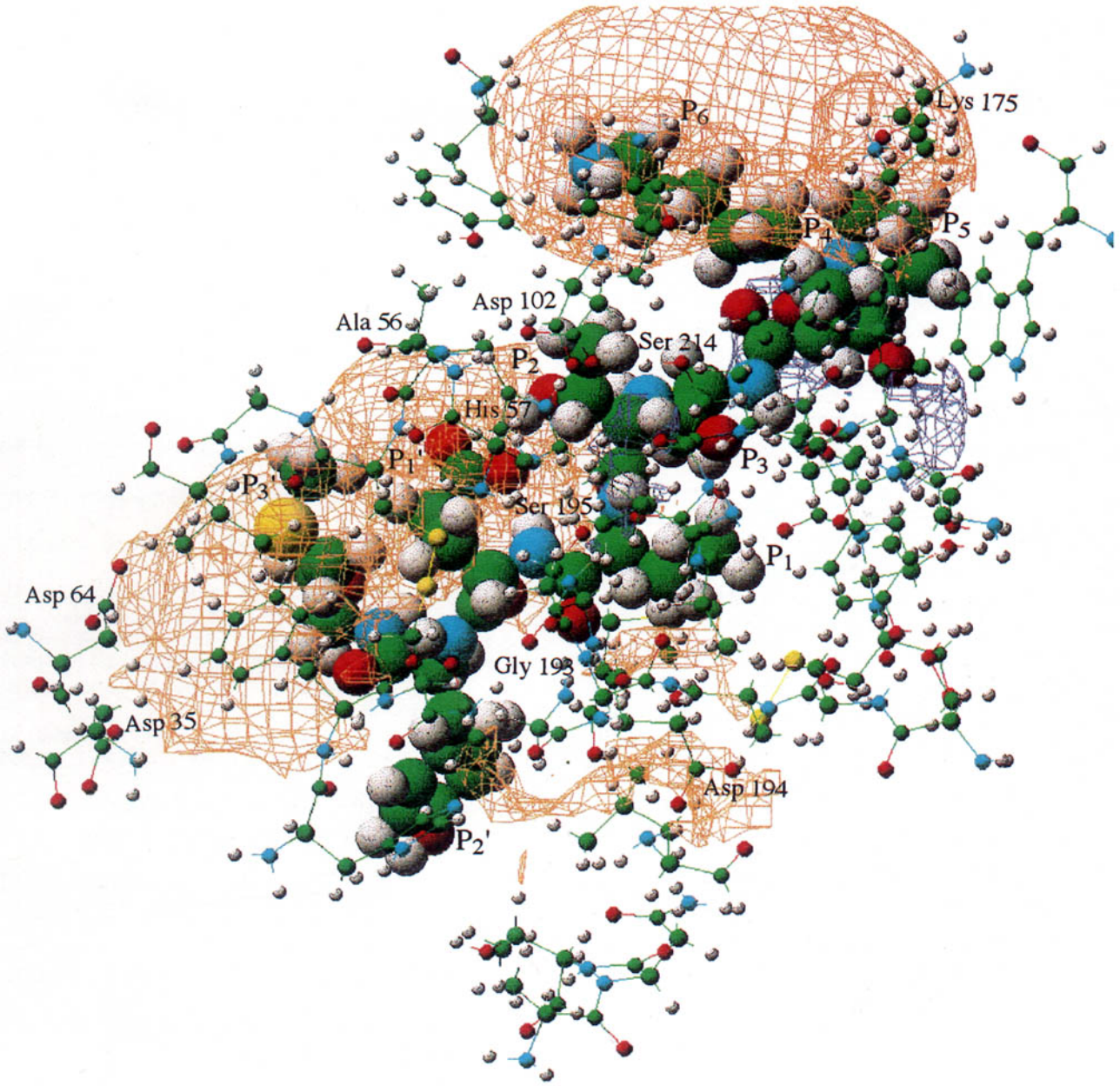

FIGURE 3. 3-D MEP correlation map of goose ovomucoid. The active site of the enzyme is shown in The ball and stick model, and the primary contact regions of goose ovomucoid are shown by the space-filling model. The colors of the atoms are same as Figure 1. Isosurfaces are same as Figure 2.

COMPLEMENTARITY AT PRIMARY RECOGNITION SITE

The primary recognition site, S_1, is said to be the hydrophobic pocket, and this is reflected in small $F_{c,res}$ and large overlapped area of solvent accessible surface at P_1 of turkey ovomucoid. In the first comparison of the primary recognition residue, P_1, between leusine and methionine (turkey–silver pheasant), the differences of $E_{c,res}$, $F_{c,res}$, and the overlapped area of the solvent accessible surface are quite small. Hence, the difference of the complementarities between turkey and silver pheasant was not observed; the replacement of leusine into methionine at P_1 has little effect on the complementarity. It is consistent with the K_a values of these ovomucoids.

On the other hand, a large difference of the hydrophobic complementarity was observed for the replacement of methionine into valine (duck and goose). It makes the $F_{c,res}$ value in this region large, and it also causes the reduction of the overlapped area. Consequently, a large reduction of the hydrophobic complementarity is brought about by valine at P_1. Similarly, valine at P_1 is more unfavorable for the hydrophobic interaction than is leusine in rhea. Hence, the goose ovomucoid has no advantage in the hydrophobic interaction at P_1, and it has the smallest K_a value of the three ovomucoids which have methionine at P'_3.

Summary

We could understand the electrostatic and hydrophobic complementarities between the enzyme and the binding site of the inhibitors using MEPs and MEP correlation. For the eight ovomucoid third domains, the MEP correlation was evaluated and compared with the binding association constant, K_a. A large difference of the electrostatic complementarity was seen in the P'_3 and P_4 positions and that of the hydrophobic complementarity was seen in the P_1 and P'_2 positions. These differences could be elucidated well by the MEP correlation of each residue, $E_{c,res}$ and $F_{c,res}$, and the aid of the overlapped area of the solvent-accessible surface, and the differences in the K_a values could be explained correctly. Arginine introduced at P'_3 gives rise to large electrostatic stabilization in this region, and it strongly promotes the binding process. Aspartate at P_4 also promotes the binding process due to an increase of the electrostatic complementarity. On the other hand, aspartate at P'_2 and alanine at P_1 ruin the hydrophobic complementarity in these regions, and it causes the large reduction of the K_a value of chicken ovomucoid. The replacement into valine at P_1 lowers the hydrophobic complementarity in this region, and it makes the K_a value of goose ovomucoid lower than that of duck and rhea ovomucoids. The present analysis of the enzyme–inhibitor interactions becomes possible by using our method which evaluates MEP of large molecular systems rapidly. Our approach was demonstrated to be effective in the analysis of the enzyme–substrate interactions and to be an effective molecular modeling tool, especially in drug design and protein engineering.

References

1. B. S. Hartley, Ann. N.Y. Acad. Sci. **227**, 438 (1974); D. M. Blow, Acc. Chem. Res. **9**, 145 (1976); J. Kraut, Annu. Rev. Biochem. **46**, 331 (1977); A. L. Fink, in *Enzyme Mechanisms*, M. I. Page and A. Williams, Eds. (The Royal Society of Chemistry, London, 1987), p. 159.
2. A. R. Fersht, *Enzyme Structure and Mechanism* (W. H. Freeman, New York, 1984).
3. B. W. Matthews, P. B. Sigler, R. Henderson, and D. M. Blow, Nature **214**, 652 (1967); J. J. Birktoft and D. M. Blow, J. Mol. Biol. **68**, 187 (1972).
4. R. J. Read and M. N. G. James, in *Protease Inhibitors*, A. J. Barrett and G. Salvesen, Eds. (Elsevier, Amsterdam, 1986), p. 301.
5. W. Bode and R. Huber, Eur. J. Biochem. **204**, 433 (1992).
6. M. Laskowski, Jr. and I. Kato, Annu. Rev. Biochem. **49**, 593 (1980).
7. W. Ardert and M. Laskowski, Jr., Biochemistry **24**, 5313 (1985).
8. M. W. Empie and M. Laskowski, Jr., Biochemistry **21**, 2274 (1982).
9. M. Laskowski, Jr., I. Kato, W. Ardert, A. Denton, M. W. Empie, W. J. Kohr, S. J. Park, K. Parks, B. L. Schatzley, O. L. Schoenberger, M. Tashiro, G. Vichot, H. E. Whatley, A. Wieczorek, and M. Wieczorek, Biochemistry **26**, 202 (1987).
10. I. Kato, J. Schrode, W. J. Kohr, and M. Laskowksi, Jr., Biochemistry **26**, 193 (1987).
11. M. Fujinaga, A. R. Sielecki, R. J. Read, W. Ardelt, M. Laskowski, Jr., and M. N. G. James, J. Mol. Biol. **195**, 397 (1987).
12. J. Avery, Int. J. Quantum Chem. **26**, 843 (1984).
13. R. Bonaccorsi, E. Scrocco, and J. Tomasi, J. Chem. Phys. **52**, 5270 (1970).
14. E. Scrocco and J. Tomasi, Adv. Quantum Chem. **11**, 115 (1978); P. Politzer and D. G. Truhlar, Eds., *Chemical Applications of Atomic and Molecular Electrostatic Potentials* (Plenum, New York, 1981).
15. G. Naray-Szabo and G. G. Ferenczy, Chem. Rev. **95**, 829 (1995).
16. H. Nakamura, K. Komatsu, S. Nakagawa, and H. Umeyama, J. Mol. Graph, **3**, 2 (1985); H. Nakamura, K. Komatsu, and H. Umeyama, J. Phys. Soc. Jpn. **54**, 3257 (1985).
17. P. Nagy and G. Naray-Szabo, Can. J. Chem. **63**, 1694 (1985); G. Naray-Szabo and P. Nagy, Enzyme **36**, 44 (1986).
18. J. S. Murray and P. Politzer, J. Org. Chem. **56**, 6715 (1991); J. S. Murray and P. Politzer, J. Org. Chem. **56**, 3735 (1991); P. Politzer, P. Lane, J. S. Murray, and T. Brinck, J. Phys. Chem. **96**, 7938 (1992).
19. D. M. Hays and P. A. Kollman, J. Am. Chem. Soc. **98**, 3335 (1976); D. M. Hays and P. A. Kollman, J. Am. Chem. Soc. **98**, 7811 (1976); R. P. Sheridan and L. C. Allen, J. Am. Chem. Soc. **103**, 1544 (1981); G. Naray-Szabo, Int. J. Quantum Chem. **22**, 575 (1982); H. Nakamura, M. Kusunoki, and N. Yasuoka, J. Mol. Graph. **2**, 14 (1984); K. Akahane, T. Kamijo, K. Iizuka, T. Taguchi, Y. Kobayashi, Y. Kiso, and H. Umeyama, Chem. Pharm. Bull. **36**, 3447 (1988).
20. K. Komatsu, H. Nakamura, S. Nakagawa, and H. Umeyama, Chem. Pharm. Bull. **32**, 3313 (1984).

21. O. Kikuchi, K. Horikoshi, and O. Takahashi, J. Mol. Struct. (Theochem) **256**, 47 (1992); O. Kikuchi, H. Nakajima, K. Horikoshi, and O. Takahashi, J. Mol. Struct. (Theochem), **285**, 57 (1993);
22. H. Nakajima, O. Takahashi, and O. Kikuchi, J. Comput. Chem. (in press).
23. W. J. Hehre, R. F. Stewart and J. A. Pople, J. Chem. Phys. **51**, 2657 (1969).
24. J. Ramstein and R. Lavery, Proc. Natl. Acad. Sci. U.S.A. **85**, 7231 (1988); V. Daggett, P. A. Kollmann, and I. D. Kunitz, Biopolymers, **31**, 285 (1991).
25. G. E. Schlz and R. H. Schrmer, *Principles of Protein Structure* (Springer-Verlag, New York, 1979).
26. C. Chothia, Nature **248**, 338 (1974); C. Chothia, Nature **254**, 304 (1975); C. Chothia and J. Janin, Nature **256**, 705 (1975).
27. B. Lee and F. M. Richards, J. Mol. Biol. **55**, 379 (1971).
28. I. Schechter and A. Berger, Biochem. Biophys. Res. Commun. **27**, 157 (1967); I. Schechter and A. Berger, Biochem. Biophys. Res. Commun. **32**, 898 (1968).
29. M. J. S. Dewer, E. G. Zoebisch, E. F. Healy, and J. J. P. Stewart, J. Am. Chem. Soc. **107**, 3902 (1985).
30. A. Warshel, G. Naray-Szabo, F. Sussman, and J.-K. Hwang, Biochemistry **28**, 3629 (1989).
31. U. De. V. Bidlingmeyer, T. R. Leary and M. Laskowski, Jr., Biochemistry **11**, 3303 (1972).